JOURNAL OF GEOPHYSICAL RESEARCH, VOL. 106, NO. A4, PAGES 5731–5742, APRIL 1, 2001

Three-dimensional observations of gyrating ion distributions far upstream from the Earth's bow shock and their association with low-frequency waves

K. Meziane,[1] C. Mazelle,[2] R. P. Lin,[1] D. LeQuéau,[2] D. E. Larson,[1] G. K. Parks,[3] and R. P. Lepping[4]

Abstract. This report discusses the nature of gyrating ion distributions observed on board the Wind spacecraft by the three-dimensional ion electrostatic analyzer with high geometrical factor (3DP PESA-High). The gyrating ion distributions are observed near the inner ion beam foreshock boundary at distances between ~9 and ~83 R_E. Our upstream measurements confirm several features previously reported using two-dimensional measurements. These distributions are observed in association with low-frequency waves with substantial amplitude ($|\delta \mathbf{B}|/B > 0.2$). The analysis of the waves shows that they propagate in the right-hand mode roughly along the background magnetic field. The ions are bunched in gyrophase angle when the associated waves are quasi-monochromatic and high in amplitude. The peak of the ion distribution function rotates in the gyrophase plane. If the wave train is nonmonochromatic, the particle phase angle distribution is extended over a larger range, suggesting the occurrence of a phase mixing effect or a source at the shock. The phase angle distribution also seems to be energy-dependent, and no gyrophase rotation is observed in this case. Furthermore, we have characterized the ion distributions by computing their densities as well as parallel and perpendicular velocities. The results clearly indicate that the waves are cyclotron-resonant with the field-aligned beams observed just upstream. The resonance condition strongly suggests the local production of these gyrating ions in a field-aligned-beam disruption. Such a resonant wave-particle interaction may be a dominant characteristic of the back-streaming ion population in the foreshock at large distances from the Earth's bow shock.

1. Introduction

The Wind spacecraft carries several instruments allowing detailed solar wind measurements. Since it was launched on November 1, 1994, Wind has been a relatively large distance from the Earth (up to ~200 R_E) and has crossed the Earth's bow shock many times. This allows for investigation of the foreshock region at larger distances than were studied by the ISEE and Active Magnetospheric Particle Tracer Explorers (AMPTE) spacecrafts, thereby providing the opportunity to study the association between upstream populations and wave activity at large distances from the bow shock. The evolution of the back-streaming ion distributions relative to distance from the shock can also be investigated.

Several types of upstream ion distributions in the Earth's foreshock have been identified and studied in the last two decades [*Gosling et al.*, 1978; *Paschmann et al.*, 1981]. These studies have stimulated theoretical investigations and simulations to explain the origin and properties of these populations [*Schwartz et al.*, 1983; *Gurgiolo et al.*, 1983; *Lee and Skadron*, 1985; *Schöler*, 1990]. The reflected beam and the diffuse populations represent the two limits of the observed ion distributions. The ion beams are characterized by a narrow angular distribution collimated along interplanetary magnetic field lines, and the ion beams are observed upstream from quasi-perpendicular shocks [*Bonifazi and Moreno*, 1981]. The diffuse ions exhibit an almost isotropic pitch angle distribution and are found upstream from quasi-parallel shocks.

Another category of ion distribution has been identified as intermediate ions; these distributions have a crescent-like shape in velocity space and are centered along the magnetic field direction. High time resolution observations have shown that many intermediate ion distributions have signatures of gyrating ions that are characterized by gyromotion around the magnetic field [*Gurgiolo et al.*, 1981; *Thomsen et al.*, 1985; *Fuselier et al.*, 1986a]. These gyrating ions are gyrophase-bunched (nongyrotropic) or nearly gyrotropic. The gyrophase-bunched ions have been observed throughout the region probed by the ISEE 1 spacecraft (up to 10-15 R_E from the bow shock), whereas the nearly gyrotropic distributions (or ring beams) are rarely observed beyond ~4 R_E from the shock [*Fuselier et al.*, 1986a]. The gyrophase-bunched ions are caused either by the reflection of the solar wind at the shock [*Gurgiolo et al.*, 1983] or by the disruption of an ion beam by waves generated by the beam-plasma instability [*Hoshino and Teresawa*, 1985; *Thomsen et al.*, 1985]. In the first case a portion of the incoming solar wind ions are specularly reflected at the shock, leading to gyrating distributions [*Gosling et al.*, 1982; *Gurgiolo et al.*, 1983]. Furthermore, the bunched ions can undergo gyrophase mixing within a few Earth radii of the shock [*Gurgiolo et al.*, 1993].

On the other hand, the propagation of a field-aligned beam can excite right-handed-resonant and nonresonant MHD waves propagating in both parallel and oblique directions with respect to the ambient magnetic field [e.g., *Gary*, 1991]. It is believed that these waves can, in turn, trap the ions and cause the gyrophase-bunched distribution observed within several Earth radii of the shock. This

[1]Space Sciences Laboratory, University of California, Berkeley.
[2]Centre d'Etude Spatiale des Rayonnements, Toulouse, France.
[3]Geophysics Program, University of Washington, Seattle.
[4]Laboratory for Extraterrestrial Physics, NASA Goddard Space Flight Center, Greenbelt, Maryland.

Paper number 2000JA900079.
0148-0227/01/2000JA900079$09.00

explains why gyrating ion populations are often associated with low-frequency MHD waves that have amplitudes which can reach a large fraction of the ambient magnetic field magnitude [*Paschmann et al.*, 1979; *Hoppe et al.*, 1981]. Since field-aligned beams can propagate deeply into the foreshock, we expect gyrophase-bunched distributions which are locally produced by a beam disruption to also be present at large distances from the shock. Finally, *Thomsen et al.* [1985] have reported one event in which the large-amplitude waves observed in the foreshock may also be excited by gyrating ions.

The gyrating distributions described above have been studied mainly by the ISEE Fast Plasma Experiement (FPE) [*Bame et al.*, 1978]. The instrument scans the ecliptic plane with a polar angle of 55°. This instrument allows a satisfactory dynamical characterization of field-aligned beams (B_Z component is generally small). Since gyrophase-bunched ions have a nonnegligible perpendicular velocity, three-dimensional (3-D) observations would provide a precise description. On the other hand, detailed analyses of waves associated with gyrating ions have not been reported.

In this paper we report observations from the Wind three-dimensional plasma (3DP) experiment of several gyrating ion distributions at distances between ~9 and ~83 R_E from the shock, and we discuss their association with low-frequency waves. We show similarities with the previous two-dimensional (2-D) observations, as well as new features appearing in the 3-D picture. We also report a detailed analysis of waves observed in association with the gyrating ion distributions. In section 2 we describe the data reduction of the 3DP measurements. In sections 3 and 5 we discuss the main characteristics of the observed distributions. The analysis of the associated low-frequency waves is given in section 4. In section 6 we discuss the properties of the reported distributions and their relationship to the waves. These properties suggest a scheme for the generation of these gyrating ions' distributions. We draw conclusions in section 7.

2. Instrumentation and Data Analysis

The 3DP experiment consists of two ion electrostatic analyzers with low and high geometric factors (PESA-Low and PESA-High), two electron electrostatic analyzers with low and high geometric factors (EESA-Low and EESA-High), and three pairs of solid state telescopes (SFT for electrons and SOT for ions). A detailed description of the 3DP experiment can be found in the work of *Lin et al.* [1995]. We are concerned primarily with the PESA-High detector, which covers energies from 80 eV to 30 keV with a resolution $\Delta E/E$~20%. The detector has a field of view of 4π sr. A full distribution is obtained on board in a one-half spin period (3 s) of the spacecraft. In normal telemetry mode one distribution is transmitted every 16 spins (every 48 s). In this case each transmitted PESA-High distribution is not a 3-s snapshot but corresponds to the accumulation of 16 measured distributions in order to improve counting statistics (the count level is generally low for the high-energy steps). In this mode the angular resolution is 5.625° in the sunward direction and 22.5° in the earthward direction. In high telemetry mode (burst mode) a complete ion distribution is transmitted every 3 s. In this case the earthward angular resolution is 45° (early in the Wind mission) or 22.5° (for later Wind orbits). The first two events reported in this paper were obtained in burst mode, whereas the other events were obtained in the normal telemetry mode.

The local solar wind parameters used in this study are taken from the moment calculations performed from the PESA-Low instrument, which monitors the solar wind. The magnetic field data used here come from the Magnetic Field Investigation (MFI) experiment [*Lepping et al.*, 1995]. The MFI experiment consists of dual, triaxial fluxgate DC magnetometers. We have used 3-s-averaged magnetic field components to investigate the association of low-frequency waves with back-streaming ions.

Because we are concerned with the back-streaming foreshock ions, we need to carefully isolate this population from the solar wind and other sources of contamination. We have estimated a "typical mean count level" for each energy step and angular bin of the PESA-High analyzer during selected time intervals when the Wind spacecraft was outside the foreshock. These measurements include counts from the solar wind distribution, contamination counts (caused by sunlight), and detector background noise. The selected time interval has been chosen as close as possible to the time of interest to avoid changes in the solar wind conditions. The obtained total mean count rates are then subtracted from the suprathermal distribution functions. Only background-subtracted count rates greater than 3 standard deviations above the mean count level have been included in our database of suprathermal distributions.

The fluctuations in the wave magnetic field have been studied with the minimum variance technique [e.g., *Sonnerup and Cahill*, 1967]. The usual convention is used to order the eigenvalues of the covariance matrix of the field perturbations $\lambda_1>\lambda_2>\lambda_3$ (maximum, intermediate, and minimum variances, respectively). The direction of minimum variance gives the direction of propagation with respect to the background magnetic field $\mathbf{B_0}$, computed as the averaged field vector during the time interval, and provides the angle θ_{kB} between the wave vector $\mathbf{k}$ and $\mathbf{B_0}$. If one assumes that λ_3 represents isotropic background noise, the error of this determination can be estimated by $\Delta\theta_{kB} = \mathrm{atan}(\lambda_3/\lambda_2-\lambda_3)$ [*Hoppe et al.*, 1981]. The polarization of the field perturbation can be determined with respect to the ambient field $\mathbf{B_0}$ in the spacecraft frame. The fluctuating levels of the magnetic field and the solar wind proton perturbations can then be computed, as, for example, the magnetic field compression ratio $\delta|\mathbf{B}|/B_0$, the proton density compression ratio $\delta N_P/N_P$ and the ratio $\delta|\mathbf{B}|/B_0$, which characterizes the amplitude of the wave field.

3. Observations

In this section we present six events associated with the gyrating-like distributions. Events a and b were observed in burst mode whereas events c - f are observed in normal telemetry mode.

3.1. Event a: April 16, 1996, 2034 - 2037 UT

Figure 1 shows 2.0-28 keV (Figure 1a) ion fluxes measured by the PESA-High analyzer in low telemetry mode (48-s time resolution) on April 16, 1996, between 2030 and 2100 UT. Figures 1b-1e show 2.6-6.4 keV ion fluxes obtained in burst mode (3 s), between 2034 and 2037 UT. The solar wind counts have been removed assuming that the main solar wind counts lie mainly within a 22.5° by 22.5° square centered on the Sun-Earth direction. The remaining fluxes are primarily due to back-steaming ions. The dashed horizontal line in Figures 1b-1e corresponds to the averaged instrumental background and contamination flux level. The available high time resolution ion measurements are partly obtained during the onset phase of an upstream event (times indicated by the two horizontal bars on Figure 1a). Figures 1f and 1g show the z component of the solar wind velocity and the solar wind density as measured by the PESA-Low analyzer. In all panels of Figure 1, oscillations appear simultaneously for all measured quantities. The

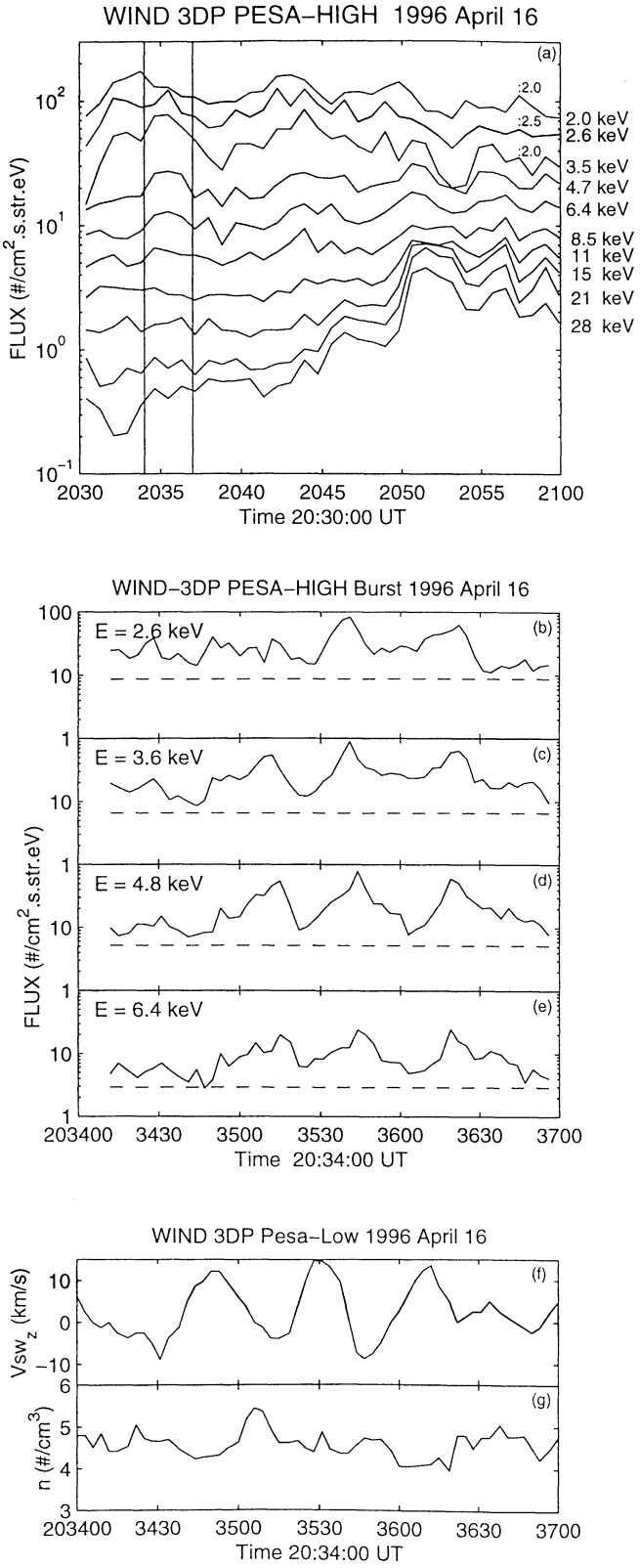

Figure 1. (a) The 2-28 keV ion fluxes measured by the PESA-High analyzer on April 16, 1996, between 2030 and 2100 UT. The two vertical bars indicate where the high time measurements are available. For clarity, the 2.0, 2.6, and 3.5 keV fluxes have been multiplied by factors of 2, 2.5, and 2, respectively. (b-e) Samples of the high time resolution ion fluxes between 2.6 and 6.4 keV. (f) The z component of the solar wind velocity and (g) the solar wind density as measured by the PESA-Low analyzer.

GSE coordinates of Wind at those times were 11.9, 34.7, and -3.5 R_E.

The following is an examination of the ion distributions associated with the event. In order to demonstrate the capabilities of the instrument, we display the three-dimensional distributions in the solar wind frame of reference. Plate 1 displays 3-s snapshots of the distribution measured at different times for the 3.6- and 2.6-keV energy channels. The ion energy spectrum maximum is in these channels. The most suitable frame for representing gyrating ion distributions is a frame related to the magnetic field. We use the Hammer-Aitoff equal area projection to display the 4π sr angular coverage (see Appendix A). The solid lines indicate the pitch angle values: the dot at the center corresponds to a value of 180° (or **-B** direction), and successive lines are separated by an angle of 30° in pitch angle. Finally, we note that the interplanetary magnetic field (IMF) direction used to plot the distribution function is averaged over the entire interval. Plate 1 clearly indicates ions propagating sunward (pitch angle > 90°, because **B** is oriented earthward). At 2034:19 UT the distributions show an ion beam propagating roughly along the **-B** direction. At 2034:28 UT the peak of the ion beam distribution shifts toward a pitch angle of ~135°. On the next snapshot at 2034:31 UT the ion distribution again becomes field-aligned. At 2034:37 UT the ion distribution peaks at non-zero pitch angle for both energy channels. It is also clear that the beam is moving around the ambient IMF direction. For this time interval the angular resolution is 45° earthward, thus the gyration appears in 45° steps. The gyration period is ~40 s, similar to the period of the oscillations observed in the plasma and magnetic field data (section 4). Also, the motion appears quasi-linear and left-handed in the solar wind frame. The same pattern is observed for ions of 2, 4.8, and 6.4 keV. At higher energies the statistics are worse. Between 2035:09 and 2036:15 UT the ion distribution is relatively narrow in gyrophase; the particle gyrophase range seems independent of the ion energy. However, after 2036:15 UT the ion distribution has a broader gyrophase region and sometimes appears with two symmetrical "bunches" as in 2036:31 and 2036:50 UT. In this case the organization in gyrophase depends upon the energy. This change in gyrophase organization seems to coincide with time periods where the particle flux oscillation is less obvious.

3.2. Event b: October 27, 1998, 0112 - 1217 UT

Plate 2 shows successive 3-D ion distribution snapshots for 6.5- and 4.8-keV energy channels as measured on October 27, 1998, between 0114:16 and 0114:45 UT. Each snapshot is obtained during a 3-s interval in burst mode. The angular resolution is 22.5° in the earthward direction and higher in the sunward direction. As in the above interval, the IMF direction used to plot the distribution function is an value averaged over the entire interval. At 0114:16 UT the ion distribution shows a field-aligned beam propagating upstream. Following 0114:20 UT, gyrating ions are identified. The particle gyrophase range is energy-dependent between 0114:20 and 0114:35 UT. The distributions measured between 0114:38 and 0114:45 UT display a narrow gyrophase angle. No gyrophase motion is observed during a substantial fraction of the wave period (Table 3) as obtained from the analysis of waves observed in association with the event (section 4).

3.3. Event c: December 11, 1994, 1251 - 1256 UT

We present here an event obtained in normal telemetry mode. The ion distribution was measured on December 11, 1994 between 1251 and 1255 UT while Wind was at 22 R_E from the shock. We have averaged the magnetic field data over the accumulation inter-

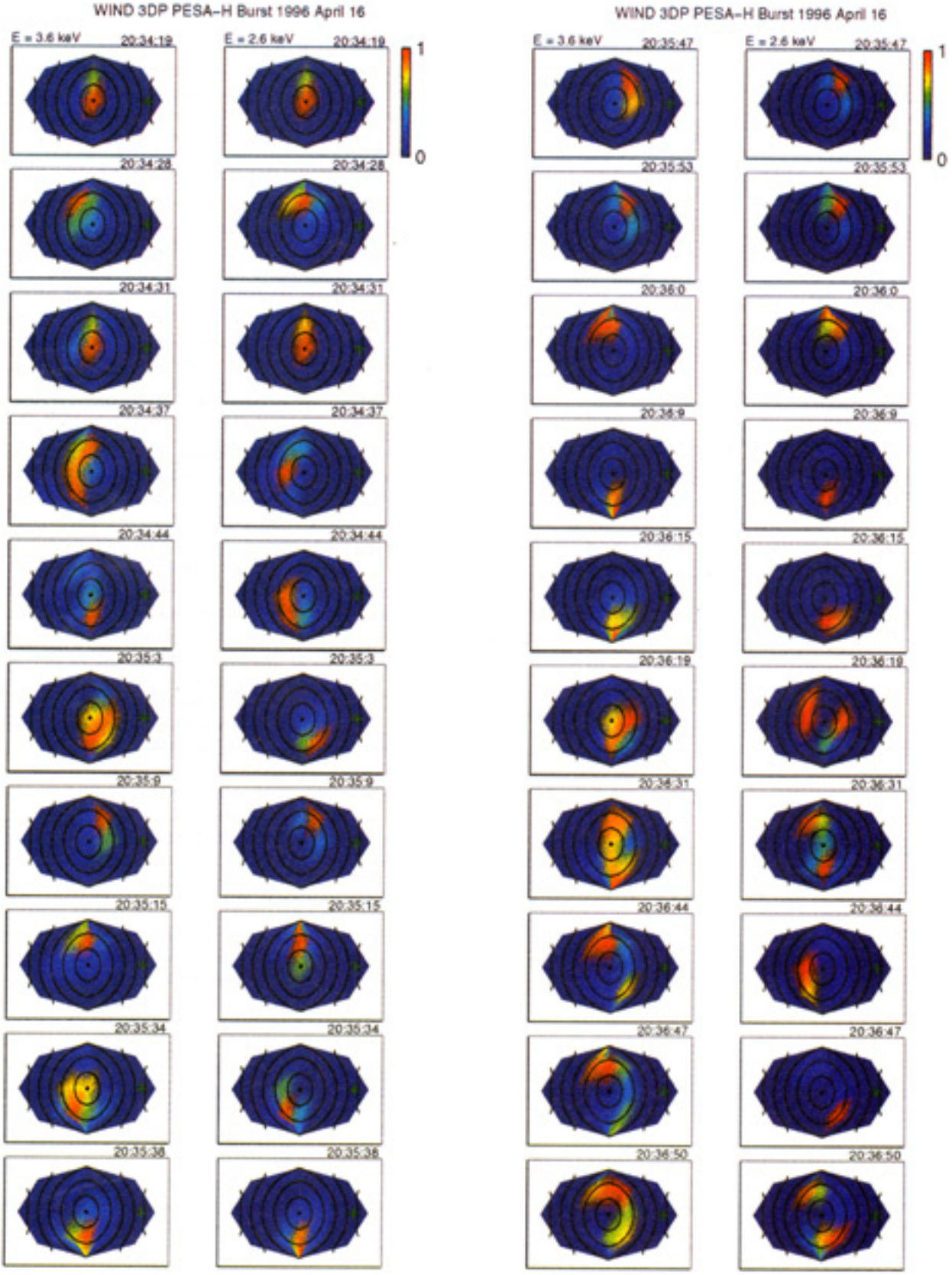

Plate 1. Three-dimensional 3-s snapshots of ion angular distributions for 3.6 and 2.6 keV. Each sphere is projected to display 4π coverage. The **-B** vector is located at the center of each plot. The contour plots indicate the pitch angle isovalues; two succesive contours are separated by 30° in pitch angle, and the plus sign indicates the solar wind direction. Each plot represents the normalized distribution function on a surface of constant energy in the solar wind frame of reference.

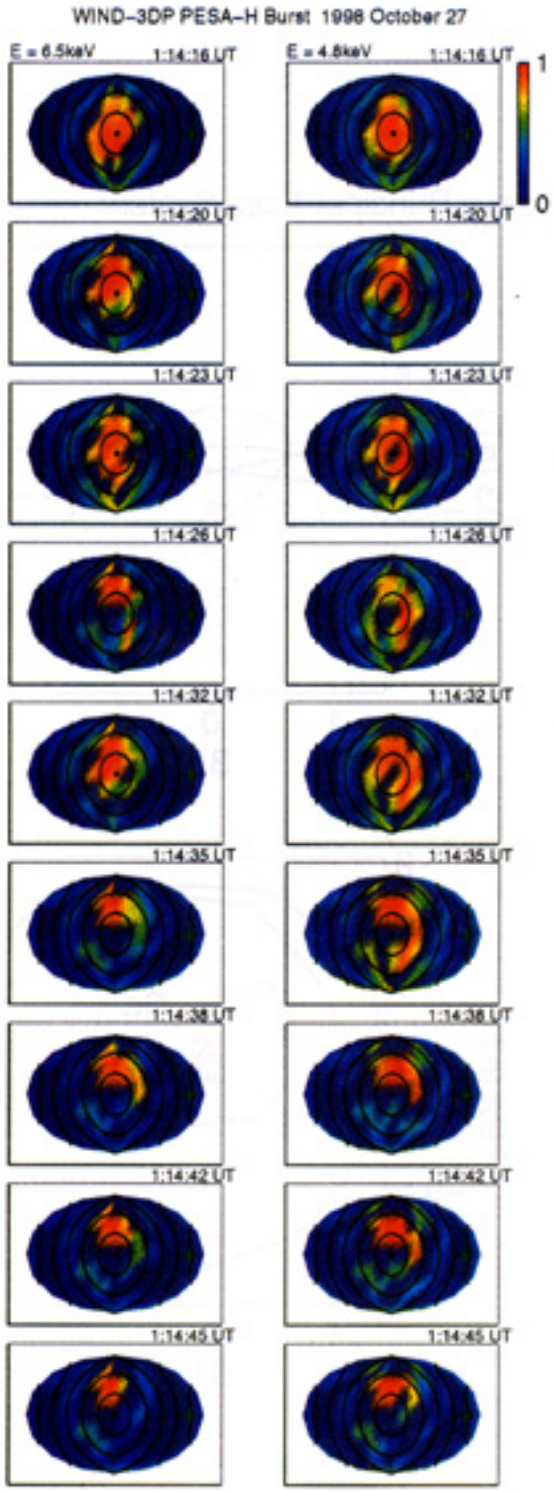

Plate 2. Same as in Plate 1. In this case the ion distributions are sampled for 6.5 and 4.8 keV; the center of each angular distribution indicates the **+B** direction.

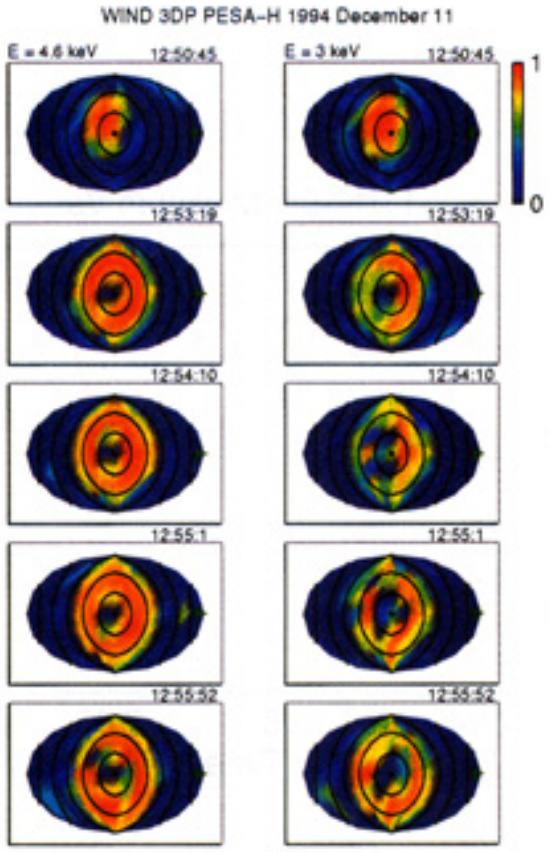

Plate 3. Three-dimentional 48 sec snapshots ion angular distributions for 4.6 keV and 3.0 keV registered on 1994 December 11. The center of each angular distribution indicates the **+B** direction.

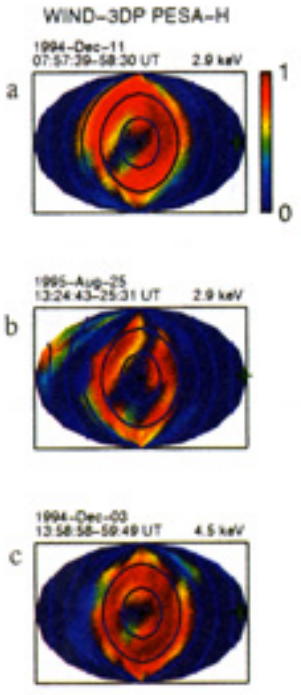

Plate 4. Same as in Plate 3 for three other ion distributions.

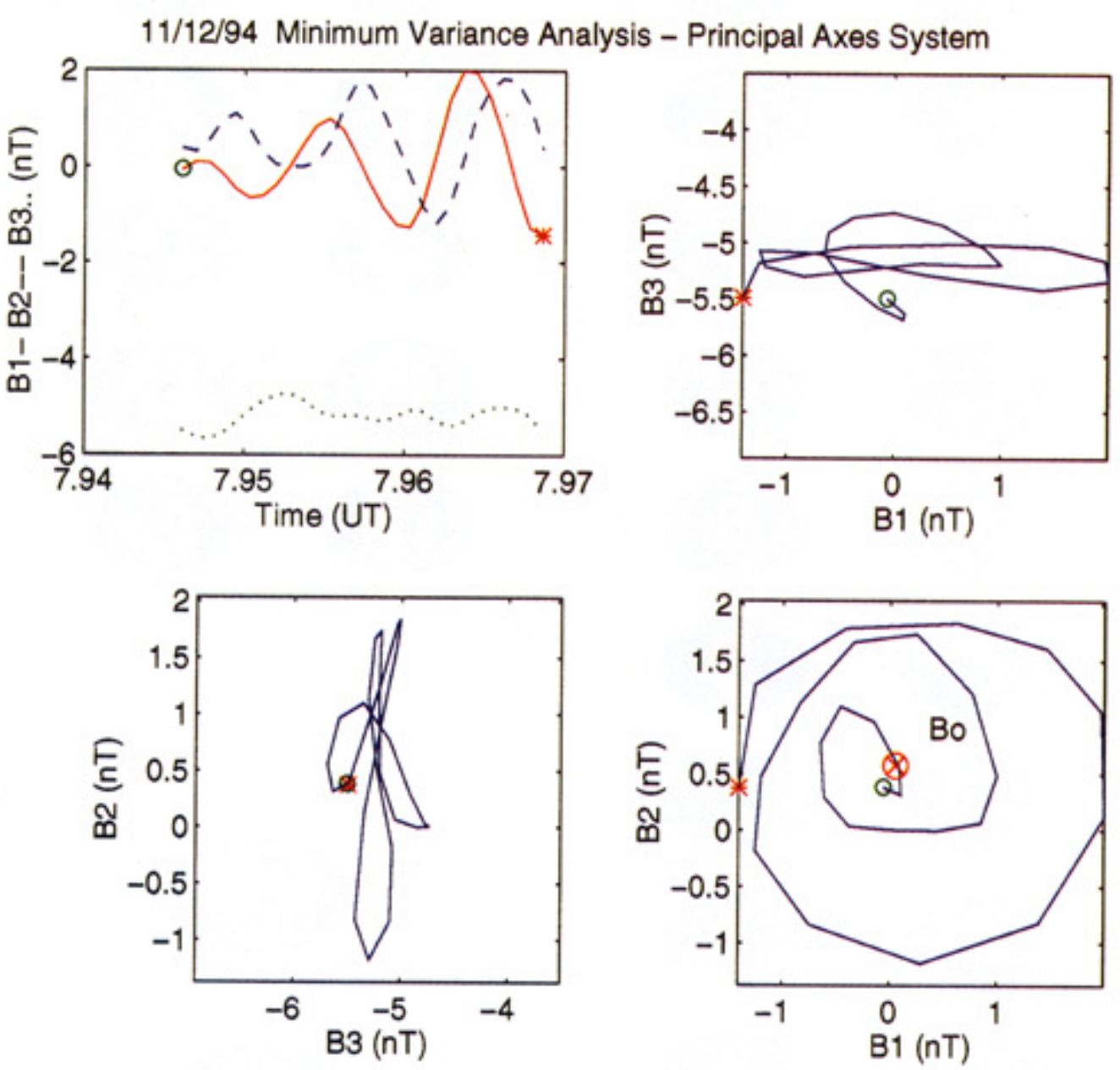

Plate 5. (a-d) Hodograms for the wave data observed in association with the ion distribution of event d. The wave is circulary left-handed-polarized in the spacecraft frame and propagates at an angle of 6° relative to the ambient magnetic field.

val of each distribution (48 s) to determine the characteristics of the back-streaming ion distributions. The averaged IMF intensity during this interval is ~6.5 nT, implying a proton gyroperiod of ~10 s. The distribution functions sampled in Plate 3 are obtained within almost five cyclotron periods. However, if the gyrating ion distribution is present thoughout a relative big time interval, as in event a, a gyrating ion population could be identified even for an integration time higher than one cyclotron period. The information about the gyrotropy, however, is lost. Plate 3 shows five consecutive distribution function snapshots for 4.6 and 3.0 keV. The snapshots measured at 1250:45 UT indicate that the ion distribution is associated with ions propagating nearly along the IMF direction. From 1253:19 to 1255:52 UT the ion distribution signature is a gyrating-like distribution. The 4.6-keV ion distribution exhibits a ring beam-like distribution, whereas the 3.0-keV particle gyrophase distribution changes from a partial ring beam between 1253:19 and 1254:10 UT to a nearly ring-beam distribution. The nearly gyrotropic appearance of these distributions may be due to the superposition of a quasi-steady gyrophase-bunched distribution rotating in the gyrophase plane as in the event a. These distributions are not observed sporadically; the shape of the distribution is remarkably steady from one 48-s sampling interval to another. This can be the case for a time interval up to ~20 proton gyroperiods, indicating a local stability of the ion distribution while the spacecraft is basically at rest. The gyrophase-bunched ion events that have been reported by *Fuselier et al.* [1986b] using ISEE 1 data are consistent with these observations.

3.4. Events d - f

Other examples of gyrating-like ion distribution functions identified at various distances from the shock are also shown in Plate 4: On December 11, 1994, at 0757:39 UT (top plot), on August 25, 1995, at 1324:43 UT (middle plot), and on December 3, 1994, at 1358:58 UT (bottom plot). The 3-D ion distributions for events d and e are given for 2.9 keV, whereas the distribution function for event f is sampled for 4.5 keV, near the peak of the ion distributions. The distributions for events d - f are similar to that for event c. The nearly ring-like distribution may also be due to a superposition of nongyrotropic ion distributions. In order to compare them with 2-D representations of gyrating ion distribution [*Gosling et al.*, 1982; *Thomsen et al.*, 1985; *Fuselier et al.*, 1986a], we have sampled one of the ion distributions in the V_X -V_Y GSE plane (V_Z = 0 plane). We choose the distribution for event e where the IMF direction lies nearly along the X_{GSE} axis (B_X = -5.3 nT, B_Y = +0.43 nT, and B_Z = +0.78 nT). To do so, we have considered angular sectors with the associated polar angle situated between 0° and 25°. Figure 2 shows a contour plot in the V_X -V_Y plane of the ion distribution for event e sampled in the solar wind frame of reference. This conventional representation of gyrating ion distribution has been used by several authors to identify gyrating ions [*Gosling et al.*, 1982; *Fuselier et al.*, 1986a] using 2-D measurements. In Figure 2, the pair of contour plots is associated with the back-streaming ions moving in the sunward direction. This cut of the back-streaming ion distribution in the V_X -V_Y plane appears to be nearly symmetrical about the mean magnetic field direction, consistent with the torus-like distribution around the magnetic field direction appearing in Plate 4. Obviously, we are not able to confirm whether or not the distribution is really gyrotropic, because the time resolution of the accumulated measured distributions is longer than the proton gyroperiod. A nongyrotropic ion distribution displays one-side contours in velocity space with respect to the magnetic field. As our measurements are integrated on a time greater than the proton gyroperiod, the distribution may represent a superposition of two single-side contours and then appears nearly gyrotropic.

4. Low-Frequency Wave Activity

Figure 3 shows the three components of the magnetic field in the GSE coordinates during intervals including the time when the ion distributions of events a, b, and d were observed. Field-aligned ion beams are observed on April 16, 1996, from 2034:20 to 2034:30 UT, and on December 11, 1994, between 0755:05 and 0757:39 UT (field-aligned beams not shown). The magnetic oscillations are relatively weak when the field-aligned beams are present. This is also the case on December 11, 1994, before 1253:19 UT (Plate 2). Also, no magnetic oscillations are associated with the observed field-aligned beams on October 27, 1998 between 0113:50 and 0114:20 UT. Large-amplitude low-frequency oscillations appear simultaneously with gyrating-like ion distributions. The waves are displayed mainly in the B_Y and B_Z components with typical peak-to-peak amplitudes of 3 nT. Plate 5 displays the results of the analysis outlined in section 2 for the distribution of event d. Plate 5a shows the time sequences of the magnetic field components in the principal axes coordinate system and the corresponding hodograms. The wave pattern is regular and quasi-monochromatic and appears strongly planar (λ_2/λ_3 = 10.4). The direction of minimum variance is therefore well defined and gives a direction of propagation nearly parallel to the ambient magnetic field $\mathbf{B_0}$, $\theta_{kB} = 6°$and within $\Delta\theta_{kB} = 6°$. The field perturbation is nearly circularly polarized (λ_1/λ_2 = 1.3) and left-hand-polarized with respect to $\mathbf{B_0}$ in the spacecraft frame, as shown on the hodogram in the principal variance plane (Plates 5b and 5d). We must emphasize that these characteristics are very robust if we

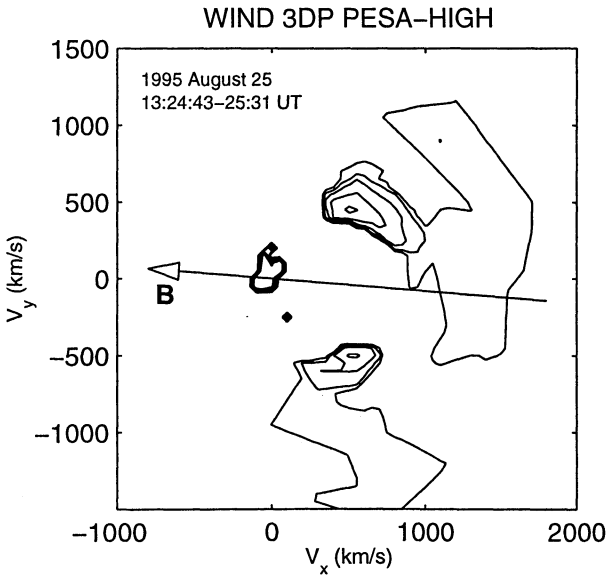

Figure 2. Contour plots of constant ion velocity distribution observed on August 25, 1995, at 1324:43-2531 UT. The arrow gives the projection of the interplanetary magnetic field (IMF) direction in the ecliptic plane. The distribution function is sampled in the plasma rest frame and in the plane $V_Z \sim 0$. The contour plots at the origin represent the solar wind. The suprathermal ion distribution consists of a pair of contours nearly symmetric about the magnetic field direction, indicating the gyrotropic-like nature of the distribution.

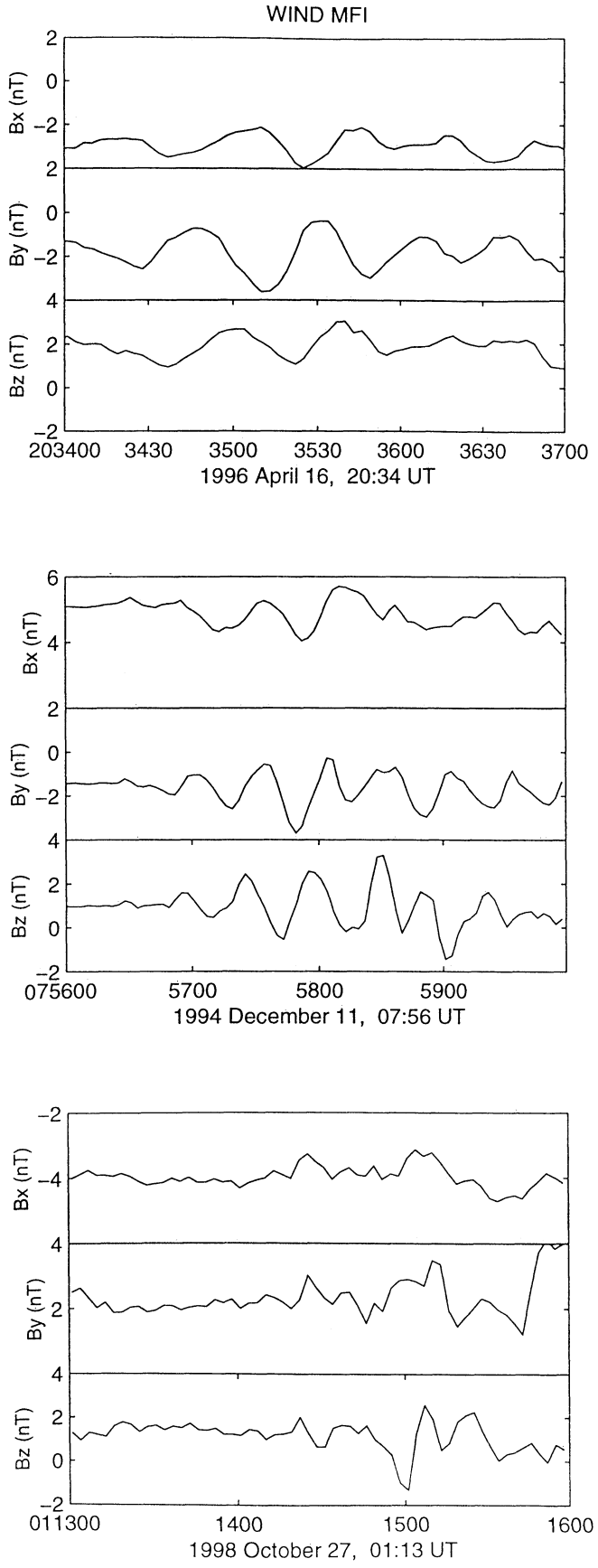

Figure 3. Magnetic field data in GSE coordinates for the time interval where the distributions of events a, b, and d have been observed.

change the time interval for the analysis. For instance, the results for 0759:30-0800:27 UT give λ_2/λ_3= 7.8, λ_1/λ_2=1.2, and the background magnetic field is also nearly invariant in direction for both intervals. The transverse wave amplitude is relatively large $|\delta\mathbf{B}|/B_0$~0.4), but the compressive component is not negligible with $|\delta\mathbf{B}|B_0$~$\delta N_P/N_P$~0.1.

We performed the same analysis for the ULF waves observed in regions where the other suprathermal gyrating proton distributions listed in Table 1 have been reported (listed in Table 1). Table 2 summarizes these properties. The observed periods T_{OBS} in the spacecraft frame are between 15 and 36 s, while the local proton cyclotron periods are between 10 and 17 s. The minimum variance analyses provide satisfactory eigenvalue ratios ($7.5<\lambda_2/\lambda_3<40.3$). The waves can be reasonably taken as plane waves, and the propagation direction is nearly parallel to the background field. The hodograms (not shown here) show that the waves are nearly circularly polarized. The polarization in the spacecraft frame is left-handed, except for the waves observed in association with the distribution of event b. The angle θ_{kV} between the wave vector and the solar wind velocity has been computed by using the proton velocity averaged over each time interval. This angle is always between ~130° and 180°, consistent with a propagation along the Sun-Earth line. We finally note that the polarization of the waves associated with the distribution of event b appears right-handed in the spacecraft frame. Also, the monochromatic feature of the wave train is less obvious than in other intervals.

5. Characterization

In this section we deal with the estimation of the parallel and perpendicular velocity of the back-streaming ions. The velocities are obtained by integrating the pitch angle distribution associated with each event. For each reported distribution, Table 1 gives the velocities parallel and perpendicular to the magnetic field direction, and the density ratio of the gyrophase-bunched ions to the solar wind. The local solar wind and Alfvén velocities are also indicated. Table 1 also provides the observed distance from the shock and the bow shock angles θ_{BV} and θ_{Bn} associated with these upstream ions (θ_{BV} is the angle between the IMF and the solar wind direction, and θ_{Bn} is the angle the magnetic field direction makes from the shock normal). These shock geometry parameters have been estimated by using a bow shock model [*Farris et al.*, 1991] and by assuming that the averaged magnetic field lines are straight between the Wind location and the bow shock. The distance from the shock is computed along the IMF line. The distributions are observed at distances between 9 and 83 R_E from the bow shock. Distributions of events b and f seem to be observed downstream in the quasi-parallel region ($\theta_{Bn} < 45°$). We note, however, that the θ_{Bn} and θ_{Vn} values listed in Table 1 may be misleading; the straight line approximation of the IMF lines is not quite valid over ~20 R_E. On the other hand, we note that the pitch angle values associated with each distribution are relatively close (~40°).

6. Discussion

We have reported in this paper three-dimensional measurements of gyrating ion distributions observed upstream of the Earth's bow shock. Numerous studies concerning gyrating ions have been reported in earlier investigations, mainly from ISEE 1 and 2 [*Gosling et al.*, 1982; *Thomsen et al.*, 1985; *Fuselier et al.*, 1986a] and AMPTE [*Sckopke et al.*, 1990; *Fazakerley et al.*, 1995] using two-dimensional measurements. Our measurements confirm several

features reported previously. The center of these distributions is rotating around the ambient magnetic field, and the ion fluxes are modulated with the magnetic oscillations simultaneously observed with the ions.

The three-dimensional plots of gyrating ion distributions (Plate 1) show new qualitative aspects. The observations indicate that when the waves are quasi-monochromatic with relatively high amplitudes, the ions are bunched in a moderate region of gyrophase. The ions are bunched within ~60° in gyrophase angle. However, when the wave amplitude decreases, the ion gyrophase range is extended, and sometimes the ions appear bunched in two symmetrical gyrophase domains. A gyrophase-bunched ion distribution is, in general, a source of free energy and therefore may excite low-frequency waves when interacting with the solar wind [*Gurgiolo et al.*, 1983]. A weak interaction with the solar wind causes a gyrophase-bunched ion distribution to evolve toward a nearly gyrotropic distribution due to gyrophase mixing after a few gyroperiods [*Gurgiolo et al.*, 1983]. Simulations reported by *Gurgiolo et al.* [1993] have shown that the waves excited by gyrophase-bunched ions strongly trap the ions. The process is so strong that phase mixing occurs for a substantial time period as long as the wave amplitude is sufficient to allow the trapping. The gyrating ion distributions in event a strongly support this hypothesis. The gyrophase range is larger when the monochromatic character of the waves is less obvious and the waveform appears disordered. The growing angular width in gyrophase of the bunched ions at the time of saturation may possibly represent the "detrapping" of the ions in the disordered wave field. During the wave saturation stage there is no energy transfer from the particles to the wave. The phase angle ψ between the instantaneous wave magnetic field and the perpendicular velocity of the bunched ions must then be close to 0° (parallel propagation) or 180° (antiparallel propagation) [*Gary et al.*, 1986; *Fuselier et al.*, 1986b]. In order to determine whether the above feature is valid, we have estimated the angle ψ by using the particle and wave properties of events a and b. For event a, between 2035:09 and 2036:15 UT, we have found that the angle ψ is roughtly between 201° and 218°. These values of ψ agree with the theoretical expectation of 180°, taking account of uncertainties due to the angular resolution of the measurements. For event b, we have found that the wave magnetic field and particle velocity directions are uncorrelated.

On the other hand, the wave trapping is a nonlinear but coherent interaction involving monochromatic waves and suprathermal particles. It is interesting to note that the trapping for the ion distributions reported here would occur for ~40° pitch angle. The trapped ion trajectories in the wave field have been outlined by several authors [*Gendrin*, 1974; *Le Quéau and Roux*, 1987; *Mazelle et al.*, 2000]. *Mazelle et al.* [2000] reported that the nonlinear interaction tends to create a peak in the ion distribution around trapping cells associated with the pitch angle $\alpha_0 \sim (2\delta|\mathbf{B}_\perp| / B_0)^{1/3}$. This theoretical estimation of the pitch angle agrees with the observed pitch angle associated with the the peak of the ion distributions (Table 1).

The statistical study by *Fuselier et al.* [1986a] shows that the nongyrotropic gyrating ions are observed at distances up to the ISEE 1 apogee (10-15 R_E). Only three cases of gyrotropic ions have been observed more than 4 R_E from the shock [*Fuselier et al.*, 1986a]. Nonetheless, these latter cases are localized within ~10 R_E of the shock. This suggests that the distance of ~4 R_E can be considered an effective cutoff distance for gyrating ions resulting from simple specular reflection at the shock [*Fuselier et al.*, 1986a]. In reports on the Earth's foreshock ions all gyrating ions (gyrophase-bunched) were observed from the shock up to the limit defined by the ISEE 1 spacecraft orbit. This is consistent with both shock acceleration and field-aligned beam disruption origins.

There are three pieces of evidence that support the conjecture that the most probable source for the distributions of events a, c, and d is local production. First, we have reported several gyrating ion distributions at distances greater than 20 R_E from the shock including the distribution of event f, which was observed at 83 R_E from the shock. Second, on the basis of bulk velocity calculations, we have found that the ions contributing to these distributions have their source away from the shock. In other words, the guiding center velocity for each distribution reported here is consistent neither with specular reflection at the shock surface of a portion of incident solar wind ions nor with magnetosheath leakage (the computation is meaningless for the distributions of events e and f. Third, the temporal flux profiles of the distributions of event a do not show any evidence of time delays between successive energy channels. The ion fluxes arise simultaneously at all energies. One possibility is that such distributions result from a field-aligned beam disruption [*Hoshino and Teresawa*, 1985]. This disruption is caused by MHD-like waves excited by an electromagnetic ion/ion beam-plasma instability. This instability leads to a gyrophase-bunched distribution which can propagate several Earth radii away. In agreement with earlier investigations [*Thomsen et al.*, 1985; *Fuselier et al.*, 1986a] the gyrotropic-like ion distributions reported here are always associated with highly transverse, weakly compressive, low-frequency waves propagating at small angles relative to the IMF. The waves, except those associated with the distribution of event b, are quasi-monochromatic ("pure," following the nomenclature of *Fuselier et al.* [1986a]) with large amplitudes and are noncompressive in agreement with earlier statistical studies [*Fuselier et al.*, 1986a]. Particularly for the distributions of events a, c, and d in Table 1, the properties of the associated waves imply that they could correspond to the early stage or the linear phase of wave excitation by an initial nongyrotropic distribution produced by gyrophase bunching. For a wide range of the mean pitch angle values of gyrating ions (particularly when it is moderate, which is the case here), the instability which gives rise to the largest growth rate is the ion/ion right-hand helical beam instability [e.g., *Gary*, 1991, and references therein]. This type of instability also has been reported largely around comets, generated from the newborn ions at the heavy ion gyrofrequency [e.g., *Brinca*, 1991; *Tsurutani*, 1991, and references therein] as well as at the proton gyrofrequency [*Mazelle and Neubauer*, 1993]. The generated wave mode is necessarily costreaming with the ions along the ambient magnetic field, i.e., toward the Sun, since there is no counterstreaming right-hand mode which can resonate with a back-streaming ion population ($\mathbf{k}.\mathbf{V}_{||}$ must be positive). In the MHD limit, this mode is the magnetosonic mode, and its phase velocity is of the order of the local Alfvén speed, i.e., much smaller than the parallel ion speed $V_{||}$ which is always larger than the solar wind speed V_{SW} (see Table 1). Therefore the ion beam overtakes the waves so that there is an anomalous Doppler shift in the ion beam reference frame: The ions sense left-handed waves. Considering the small spacecraft velocity relative to the Earth, the proton right-hand mode waves are also observed in the spacecraft frame as left-handed waves [*Hoppe and Russell*, 1983]. Moreover, for the MHD limit of this type of low-frequency (magnetosonic) waves, the group velocity is parallel to the magnetic field with the same sense as $\mathbf{k}_{||}$. Therefore the wave energy (the Poynting flux) is driven away from the Earth's environment in the solar wind frame, toward the Sun, in contrast to solar wind originated waves. This is

Table 1. Gyrating Ion Density, Parallel and Perpendicular Velocities, and Distance from the Shock

Event	$V_{\|\|}$, km/s	$V_{\perp}$, km/s	n_p/N_P, %	V_{SW}, km/s	V_A, km/s	D, R_E	θ_{BV}, deg	θ_{Bn}, deg
(a) April 16, 1996 2035:09 UT	600	510	0.40	450	42	17	46	42
(b) Oct. 27, 1998 0114:35 UT	680	500	0.80	400	40	9	29	35
(c) Dec. 11, 1994 1254:10 UT	670	520	0.28	450	56	21	6	12
(d) Dec. 11, 1994 0757:39 UT	520	570	0.27	470	54	26	19	29
(e) Dec. 3, 1994 1358:58 UT	780	610	0.13	520	50	38	18	27
(f) Aug. 25, 1995 1324:43 UT	600	520	0.07	430	44	83	8	35

fully consistent with the observed values of θ_{kV}, despite the 180° ambiguity in the experimental determination of the direction of the wave vector.

To investigate quantitatively the possibility of a resonant instability, we compare the observed wave period with one we would expect for waves in cyclotron resonance with ion beams observed just upstream of gyrating ions (when the ion beams are observed). The distributions observed farthest from the shock, events e and f, are not included in this analysis because they are not observed near field-aligned beams. The resonance condition is

$$\omega - k_{\|} V_{\|} + \Omega_P = 0, \tag{1}$$

where ω is the wave frequency in the solar wind rest frame, Ω_P is the proton gyrofrequency, $k_{\|}$ is the component of the wave vector parallel to the background magnetic field, and $V_{\|}$ is the ion beam parallel component of the resonant ion velocity (in the solar wind frame). By assuming $\omega << \Omega_P$, we can make the approximation

$$k_{\|} \sim \Omega_P / V_{\|}. \tag{2}$$

We give the parallel wavelength $\lambda_{\|}$ of these resonant waves in Table 2. They all are of the order of 1 R_E. In the spacecraft frame, these waves would have a Doppler-shifted frequency of

$$\omega' = \omega + \mathbf{k}.\mathbf{V_{SW}} \sim k_{\|} V_{SW} \cos\theta_{kV} / \cos\theta_{kB}. \tag{3}$$

The measured values of the beam velocities are obtained from the pitch angle distribution and are given in Table 3. Using the experimental values, we have computed the predicted wave periods $T_{PRED} = 2\pi/\omega'$ according to (2) and (3) and compared them with the observed periods. Taking into account the experimental uncertainties, the observed periods are systematically close to those predicted for the distributions of events a, c, and d. This strongly supports the possibility that local cyclotron resonance occurs for these events. Moreover, the observed variations of the wave field, such as those shown by the hodograms in Plate 5, are experimental indications of a local interaction with particles of the plasma. Although a gyrating ion distribution still contains a large amount of free energy to generate a wave of this kind [e.g., *Killen et al.*, 1995], the waves are not necessarily produced by the observed distributions. Our analysis shows that the observed parallel velocities of gyrating ions (Table 1) are too small for T_{PRED} to match T_{OBS}. Therefore a possible scenario is that these waves could be generated by other ion distributions (field-aligned beams or gyrating ion distributions with similar properties) further upstream from the Earth's bow shock. These excited waves grow, propagate slightly toward the Sun in the solar wind frame, and are simply blown back past the spacecraft and the locally back-streaming particles. These waves then could be rapidly damped by resonant pitch angle scattering of the ions. Numerical simulations [*Gary et al.*, 1988] have shown that the nonlinear wave saturation occurs at small amplitudes of $|\delta\mathbf{B}|/B_0| \sim 0.25$, which is consistent with our observations.

We finally note that the event b is associated with gyrophase-bunched ions in which the gyrophase angle appears the same during the successive distributions. This event is associated with ULF waves where the monochromatic character is absent in the wave train. The wave analysis indicates that (1) the wave mode is left-handed in the solar wind frame of reference and (2) the resonance condition between the waves and the beam observed just before the gyrophase-bunched ions is not satisfied (Table 3). We suggest in this case that the waves are probably excited by other ion distributions further upstream and past the spacecraft. The absence of

Table 2. Properties of Waves Associated with Gyrating Ion Distributions

Event	λ_2/λ_3	λ_1/λ_2	θ_{kB}, deg	θ_{kV}, deg	$\|\delta\mathbf{B}\|/B$	$\delta\|\mathbf{B}\|/B$	$\delta N_P/N_P$	T_{OBS}, s	T_C, s	$\lambda_{\|}$, R_E
(a) April 16, 1994 2034:28-35:56 UT	22.6	2.5	10±3	145±3	0.46	0.18	0.18	36±4	16.6	2.00±0.11
(b) Oct. 27, 1998 0113:58-01:40 UT	11.0	1.4	22±6	131±7	0.17	0.06	0.11	15±2	14.0	0.67±0.09
(c) Dec. 11, 1994 1253:38-54:35 UT	22.6	1.9	8±3	162±3	0.22	0.05	0.10	22±4	10.0	1.49±.008
(d) Dec. 11, 1994 0756:35-58:05 UT	10.4	1.3	6±6	154±6	0.39	0.15	0.16	28±4	12.5	2.00±0.16
(e) Dec. 3, 1994 1358:44-59:20 UT	7.5	4.3	17±9	156±9	0.15	0.05	0.04	15±3	13.8	1.22±0.14
(f) Aug. 25, 1995 1322:14-23:19 UT	40.3	3.0	8±2	176±3	0.27	0.05	0.03	27±2	12.3	1.57±0.17

Table 3. Beam Velocity and Wave Periods (Observed and Predicted)

Beam	V_{beam}, km/s	T_{OBS}, s	T_{PRED}, s
April 16, 1996 2034:31 UT	-770±120	36±4	36±6
Oct. 27, 1998 0114:16 UT	750±130	15±2	25±5
Dec. 11, 1994 1250:45 UT	900±100	22±4	21±2
Dec. 11, 1994 0755:58 UT	1100±100	28±4	31±3

resonance could also indicate that the ions are generated at the quasi-parallel shock (θ_{Bn}~35°). The distribution of event b is observed at ~9 R_E from the shock, and the estimation of θ_{Bn} is more reliable than those associated with the distributions observed further from the shock. We also must emphasize that as found above, the gyrophase angle of the bunched ions is not correlated with the wave magnetic field, strongly indicating a source at the shock of the ions.

7. Conclusion

We have reported the observation of several gyrating ion distributions and the associated low-frequency waves at large distances from the shock. These gyrating ions are observed just downstream of the inner ion beam foreshock boundary. The detailed analysis performed here clearly shows the existence of wave-particle interactions. The resonant interaction between field-aligned ion beams and MHD-like waves strongly suggests that the source of the gyrating ions is the disruption of the ion beams [*Hoshino and Teresawa*, 1985]. This process is a dominant feature of the foreshock at large distances. Nevertheless, the excitation of the waves by the gyrating ions cannot be ruled out [*Thomsen et al.*, 1985], even though the wave-particle resonance is not verified. On the other hand, our data show that when the MHD-like waves are quasi-monochromatic with high amplitude, the gyrating ion distributions are highly stable; the ions are bunched in a very limited range of phase angle. The particle gyrophase range appears broader and complex when the waves are not "pure" and/or have weak amplitude. Finally, as indicated in Table 1, the gyrating ion density normalized to the solar wind density decreases with the distance from the shock. However, the distance limit of the observation of gyrating ions may be very large, suggesting that they could be observed as far upstream as relatively dense field-aligned beams.

Appendix A: The Hammer-Aitoff Projection

The Hammer-Aitoff projection is an equal-area world projection based on a spherical model of the Earth [*Mailing*, 1992]. The projection is useful to display data for mapping. It has been used to represent the celestial sphere. The sphere in this projection is represented within an ellipse with axes in a 2:1 ratio. The equator and the central meridian are straight lines whereas the rest of the parallels and meridians are curves. The curvature of the parallels is such that it reduced the angular distortion at the poles. The x axis (horizontal) is along the equator, and the y axis coincides with the central meridian. The transformation from the spherical coordinates (φ,θ) to the cartesian coordinates (x,y) is

$$x = 2k\cos\theta\sin(\varphi/2),$$

$$y = k\sin\theta,$$

where $k = \sqrt{2}/\sqrt{1+\cos\theta\cos(\varphi/2)}$, with $-\pi \le \varphi \le \pi$ and $-\pi/2 \le \theta \le \pi/2$. In the 3-D representation used in this paper, φ and θ are associated with the looking direction of the detector. Also, the transformation has been rotated in order to place the direction of the magnetic field at the center.

Acknowledgments. Michel Blanc thanks Stephen Fuselier and another referee for their assistance in evaluating this paper.

References

Bame, S. J., J. R. Asbridge, H. E. Felthauser, J. P. Glore, G. Paschmann, P. Hemmerich, K. Lehmann, and H. Rosenbauer, ISEE 1 and 2 fast plasma experiments and the ISEE 1 solar wind experiment, *IEEE Trans. Geosci. Electron., GE-16*, 216, 1978.

Bonifazi, C., and G. Moreno, Reflected and diffuse ions backstreaming from the Earth's bow shock, *J. Geophys. Res., 86*, 4397, 1981.

Brinca, A. L., Cometary linear instabilities: From profusion to prospective, in *Cometary Plasma Processes, Geophys. Monogr. Ser.*, vol. 61, edited by A. D. Johnstone, pp. 211-221, AGU, Washington, D. C., 1991.

Farris, M. H., S. M. Petrinec, and C. T. Russell, The thickness of the magnetosheath: Constraints on the polytropic index, *Geophys. Res. Lett., 18*, 1821, 1991.

Fazakerley, A.N., A.J. Coates, and M.W. Dunlop, Observations of upstream ions, solar wind ions and electromagnetic waves in the Earth's foreshock, *Adv. Space Res., 15* (8/9), 103, 1995.

Fuselier, S. A., M. F. Thomsen, J. T. Gosling, S. J. Bame, and C. T. Russell, Gyrating and intermediate ion distributions upstream from the Earth's bow shock, *J. Geophys. Res., 91*, 91, 1986a.

Fuselier, S. A., M. F. Thomsen, S. P. Gary, S. J. Bame, C. T. Bame, C. T. Russell, and G. K. Parks, The phase relationship between gyrophase-bunched ions and MHD-like waves, *Geophys. Res. Lett., 13*, 60, 1986b.

Gary, S.P., Electromagnetic ion/ion instabilities and their consequences in space plasmas: A review, *Space Sci. Rev., 56*, 373, 1991.

Gary, S. P., M. F. Thomsen, and S. A. Fuselier, Electromagnetic ion beam instabilities: Gyrophase bunched ions, *Phys. Fluids, 29*, 531, 1986.

Gary, S. P., C. D. Madland, N. Omidi, and D. Winske, Computer simulation of two-pickup-ion instabilities in a cometary environment, *J. Geophys. Res., 93*, 9584, 1988.

Gendrin, R., Phase-bunching and other nonlinear processes occuring in gyroresonant wave-particle interactions, *Astrophys. Space Sci., 28*, 245, 1974.

Gosling, J. T., J. R. Asbridge, S. J. Bame, G. Paschmann, and N. Schopke, Observations of two distinct population of bow shock ions in the upstream solar wind, *Geophys. Res. Lett., 5*, 957, 1978.

Gosling, J. T., M. F. Thomsen, S. J. Bame, W. C. Feldman, G. Paschmann, and N. Schopke, Evidence for speculary reflected ion upstream from the quasi-parallel bow shock, *Geophys. Res. Lett., 9*, 1333, 1982.

Gurgiolo, C., G. K. Parks, B. H. Mauk, C. S. Lin, K. A. Anderson, R. P. Lin, and H. Rème, Non **ExB** ordered ion beams upstream of the Earth's bow shock, *J. Geophys. Res., 86*, 4451, 1981.

Gurgiolo, C., G. K. Parks, and B. H. Mauk, Upstream gyrophase bunched ions: A mechanism for creation at the bow shock and the growth of velocity space structure through gyrophase mixing, *J. Geophys. Res., 88*, 9093, 1983.

Gurgiolo, C., H. K. Wong, and D. Winske, Low and high frequency waves generated by gyrophase bunched ions at oblique shocks, *Geophys. Res. Lett., 20*, 783, 1993.

Hoppe, M. M., and C. T. Russell, Plasma rest frame frequencies and polarization of the low frequency upstream waves: ISEE 1 and 2 observations, *J. Geophys. Res., 88*, 2021, 1983.

Hoppe, M. M., C. T. Russell, L. A. Frank, T. E. Eastman, and E. G. Greenstadt, Upstream hydromagnetic waves and their association with backstreaming ion populations: ISEE 1 and 2 observations, *J. Geophys. Res., 86*, 4471, 1981.

Hoshino, M., and T. Teresawa, Numerical study of the upstream waves excitation mechanism, 1, Nonlinear phase bunching of beam ion, *J. Geophys. Res., 90*, 57, 1985.

Killen, K., N. Omidi, D. Krauss-Varban, and H. Karimabadi, Linear and nonlinear properties of ULF waves driven by ring-beam distribution functions, *J. Geophys. Res., 100*, 5835, 1995.

Lee, M. A., and G. Skadron, A simple model for formation of reflected, intermediate and diffuse ion distributions upstream of Earth's bow shock, *J. Geophys. Res.*, 90, 39, 1985.

Lepping, R. L., et al., The Wind magnetic field investigation, *Space Sci. Rev.*, *71*, 207, 1995.

Le Quéau, D., and A. Roux, Quasi-monochromatic wave-particle interactions in magnetospheric plasmas, *Sol. Phys.*, *111*, 59, 1987.

Lin, R. P., et al., A three-dimensional plasma and energetic particle investigation for the Wind spacecraft, *Space Sci. Rev.*, *71*, 125, 1995.

Mailing, D. H., *Coordinate Systems and Map Projections*, 2nd ed., Pergamon, Tarrytown, N. Y., 1992.

Mazelle, C., and F.M. Neubauer, Discrete wave packets at the proton cyclotron frequency at comet P/Halley, *Geophys. Res. Lett.*, *20*, 153, 1993.

Mazelle, C., D. LeQuéau, and K. Meziane, Nonlinear wave-particle interaction upstream from the Earth's bow shock, *Nonlinear Processes Geophys.*, *7* (3/4), 185, 2000.

Paschmann, G., N. Schopke, S. J. Bame, J. R. Asbridge, J. T. Gosling, C. T. Russell, and E. W. Greenstadt, Association of low frequency waves with suprathermal ions in the upstream solar wind, *Geophys. Res. Lett.*, *6*, 209, 1979.

Paschmann, G., N. Schopke, I. Papamastorakis, J. R. Asbridge, S. J. Bame, and J. T. Gosling, Characteristics of reflected and diffuse ions upstream from the Earth's bow shock, *J. Geophys. Res.*, *86*, 4355, 1981.

Schöler, M., Diffuse ions at quasi-parallel collisionless shock: Simulations, *Geophys. Res. Lett.*, *17*, 1821, 1990.

Schwartz, S. J., M. F. Thomsen, and J. T. Gosling, Ions upstream of the Earth's bow shock: A theoretical comparison of alternative source populations, *J. Geophys. Res.*, *88*, 2039, 1983.

Sckopke, N., G. Paschmann, A. L. Brinca, C. W. Carlson, and H. Lühr, Ion thermalization in quasi-perpendicular shocks involving reflected ions, *J. Geophys. Res.*, *95*, 6337, 1990.

Sonnerup, B.U.O., and L. J. Cahill, Magnetopause structure and attitude from Explorer 12 observations, *J. Geophys. Res.*, *72*, 171, 1967.

Thomsen, M. F., J. T. Gosling, S. J. Bame, and C. T. Russell, Gyrating ions and large-amplitude monochromatic MHD waves upstream of the Earth's bow shock, *J. Geophys. Res.*, *90*, 267, 1985.

Tsurutani, B. T., Comets: A laboratory for plasma waves and instabilities, in *Cometary Plasma Processes, Geophys. Monogr. Ser.*, vol. 61, edited by A. D. Johnstone, pp. 189-209, AGU, Washington, D. C., 1991.

D. E. Larson and R. P. Lin, Space Sciences Laboratory, University of California, Berkeley, CA 94720-7450.

R. P. Lepping, Lab for Extraterrestrial Physics, NASA GSFC, Greenbelt, MD 20771.

D. LeQuéau and C. Mazelle, Centre d'Etude Spatiale des Rayonnements, BP 4346, 31029, Toulouse, Cedex, France.

K. Meziane, Physics Dept., Univ. of New Brunswick, P.O. Box 4400, Fredericton, New Brunswick, Canada E3B5A3. (karim@ssl.berkeley.edu)

G. K. Parks, Geophysics Program, University of Washington, Box 35160, Seattle, WA 98195.

(Received January 24, 2000; revised May 11, 2000;
accepted May 14, 2000.)